01 Jan 1992

Effect Of Strain Rate On Cold-formed Steel Stub Columns

M. Kassar

C. L. Pan

Wei-wen Yu
Missouri University of Science and Technology, wwy4@mst.edu

Recommended Citation

M. Kassar et al., "Effect Of Strain Rate On Cold-formed Steel Stub Columns," *Journal of Structural Engineering (United States)*, vol. 118, no. 11, pp. 3151 - 3168, American Society of Civil Engineers, Jan 1992.
The definitive version is available at https://doi.org/10.1061/(ASCE)0733-9445(1992)118:11(3151)

Effect of Strain Rate on Cold-Formed Steel Stub Columns

By M. Kassar,[1] C. L. Pan,[2] and W. W. Yu,[3] Fellow, ASCE

Abstract: The material properties of steel and the strength of steel members are affected by strain rate. To investigate this characteristic for compression members, 49 stub columns fabricated from 35XF sheet steel and 48 stub columns fabricated from 50XF sheet steel are studied experimentally and analytically under different strain rates. The strain rate ranged from 10^{-5} to 0.1 in./in./sec (10^{-5} to 0.1 mm/mm/s). The material properties of 35XF and 50XF sheet steels developed from previous tests are used for the evaluation of the test data obtained from the member tests using specimens fabricated from the same sheet steel. The results show that the strength of stub columns increased with the strain rate. The amount of increase is found to be dependent on the type of material, the F_u/F_y ratio, the width-to-thickness ratio (w/t) of the compression element, and the strain rate used in the tests. The effective width approach included in the American Iron and Steel Institute (AISI) specification for cold-formed steel members and in the AISI *Automotive Steel Design Manual* is utilized for the evaluation of stub column strengths using static and dynamic yield stresses corresponding to the strain rates used in the tests. It is found that better agreement can be achieved between the predicted and tested stub column strengths when using the dynamic yield stresses and considering the effect of cold work.

Introduction

The effect of impact loading and associated strain rate on the structural strength of steel columns and flexural members has been the subject of past investigations, especially during the last three decades. It was found that theoretical analyses agree well with the experimental results when taking the steel strain-rate sensitivity into account for beams (Bodner and Symonds 1962; Rawlings 1963; Aspden and Campbell 1966; Forrestal and Wesenberg 1977). Experimental and theoretical studies indicate that steel columns with large slenderness ratios tested under impact loading may sustain compressive loads in excess of the Euler critical buckling values (Meier 1945; Hoff 1965; Roberts 1972; Logue 1971). This is because the column lateral displacement under rapid loading is less than that from static conditions.

In order for the engineer to achieve a more economical design for vehicle components subjected to impact loads, the effect of strain rate may be considered as a factor in design. During a vehicle collision, the strain rates in the zones of localized deformation can be of the order of 10–100 in./in./sec (10–100 mm/mm/s). Consequently, the dynamic capacity of a steel compression member is much greater than the static value (Wierzbicki 1977). In the analysis of car components subjected to impact loads, the dynamic compressive capacity is considered to be a product of a static-crushing strength of the column and a strain-rate correction factor depending on the initial impact velocity and the sensitivity of the material to strain factor rate (Wierz-

[1]Prin. Engr., ABB Impell Corp., 1333 Butterfield Road, Suite 550, Downers Grove, IL 60515; formerly, Grad. Res. Asst., Univ. of Missouri-Rolla, Rolla, MO 65401.

[2]Res. Asst., Dept. of Civ. Engrg., Univ. of Missouri–Rolla, Rolla, MO.

[3]Curators' Prof. of Civ. Engrg., Univ. of Missouri–Rolla, Rolla, MO.

Note. Discussion open until April 1, 1993. To extend the closing date one month, a written request must be filed with the ASCE Manager of Journals. The manuscript for this paper was submitted for review and possible publication on June 13, 1991. This paper is part of the *Journal of Structural Engineering*, Vol. 118, No. 11, November, 1992. ©ASCE, ISSN 0733-9445/92/0011-3151/$1.00 + $.15 per page. Paper No. 2099.

J. Struct. Eng., 1992, 118(11): 3151-3168

bicki 1977; Wierzbicki and Abramowicz 1979; Abramowicz and Jones 1984; Mahmood and Paluszny 1984).

In cold-formed steel design, local buckling is one of the major design features because of the use of large width-to-thickness (w/t) ratios for compression elements. The effective width approach has been adopted in several specifications to predict the load-carrying capacities of structural members in buildings and other cold-formed steel structures. Because the effective width equations included in the current AISI (*Specification* 1986) specification and the *Automotive Steel Design Manual* (1986) are primarily based on the results of static tests of cold-formed steel members corresponding to a strain rate of approximately 1.7×10^{-6} in./in./sec (1.7×10^{-6} mm/mm/s), a research project was conducted at the University of Missouri–Rolla (UMR) under the sponsorship of the American Iron and Steel Institute (AISI) to study the validity of the available effective design-width equations for the design of structural members subjected to dynamic loads.

This paper presents the results of 97 stub columns having stiffened and unstiffened elements with various width-to-thickness ratios tested under different strain rates. Comparisons between the tested static and dynamic strengths are presented herein. The findings of the effect of strain rate on mechanical properties of the sheet steel used for fabricating stub columns have been discussed by Kassar and Yu (1990).

Experimental Investigation

Twenty-four box-shaped stub columns fabricated from 35XF sheet steel and 22 box-shaped stub columns fabricated from 50XF sheet steel were tested for the study of stiffened elements. The w/t ratios of stiffened elements for the specimens fabricated from these sheet steels ranged from 22.89 to 100.62. Twenty-five I-shaped stub columns fabricated from 35XF sheet steel and 26 I-shaped stub columns fabricated from 50XF sheet steel were tested for the current study of unstiffened elements. The w/t ratios of unstiffened elements ranged from 8.29 to 44.57. The specimens were grouped in four cases of w/t ratios for the stiffened and unstiffened elements. Cases A, B, C, and D represent the small, medium, large, and extra large w/t ratios, respectively. The ranges of strain rates used in the sub-column tests were from 10^{-5} to 0.1 in./in./sec (10^{-5} to 0.1 mm/mm/s). The tensile and compressive mechanical properties of 35XF and 50XF sheet steels are given in Tables 1 and 2.

TABLE 1. Average Mechanical Properties of 35XF Sheet Steel Used in Experimental Study under Different Strain Rates

Strain rate (in./in./sec) (1)	$(F_y)_c$[a] (ksi) (2)	$(F_{pr})_c$[a] (ksi) (3)	$(F_y)_t$[b] (ksi) (4)	$(F_u)_t$[b] (ksi) (5)	Elongation[b,c] (%) (6)
0.0001	29.83	17.79	32.87	49.35	38.90
0.01	31.92	20.03	36.40	51.76	36.80
1.0	36.91	–	42.37	56.63	40.90

[a]Based on longitudinal compression coupon tests.
[b]Determined from longitudinal tension coupon tests.
[c]Measured using 2-in. (5.08-cm) gage length.
Note: 1 in./in./sec = 1 mm/mm/s; 1 ksi = 6.895 MPa.

J. Struct. Eng., 1992, 118(11): 3151-3168

TABLE 2. Average Mechanical Properties of 50XF Sheet Steel Used in Experimental Study under Different Strain Rates

Strain rate (in./in./sec) (1)	$(F_y)_c$[a] (ksi) (2)	$(F_{pr})_c$[a] (ksi) (3)	$(F_y)_t$[b] (ksi) (4)	$(F_u)_t$[b] (ksi) (5)	Elongation[b,c] (%) (6)
0.0001	49.68	38.64	49.50	72.97	31.00
0.01	52.51	40.05	51.60	74.87	27.00
1.0	54.79	–	54.66	78.73	25.80

[a]Based on longitudinal compression coupon tests.
[b]Determined from longitudinal tension coupon tests.
[c]Measured by using 2-in. (5.08-cm) gage length.
Note: 1 in./in./sec = 1 mm/mm/s; 1 ksi = 6.895 MPa.

Test Specimens

The nominal thicknesses of steel sheets used for stub columns were 0.085 in. (2.2 mm) for 35XF sheet steel and 0.077 in. (2.0 mm) for 50XF sheet steel. All specimens were cold formed by a press-brake operation with a nominal inside-bend radius of 5/32 in. (4.0 mm) at corners. The length of each stub-column specimen is longer than three times the largest dimension of the cross section of specimens and less than 20 times the least radius of gyration (Galambos 1988). For all tests, corner strain gages were used to determine maximum edge strains and corresponding stresses. The paired strain gages placed at the tips of unstiffened flanges and at the middle of stiffened flanges were used to determine the strains for critical local buckling loads by using the modified strain-reversal method (Johnson and Winter 1966).

Box-Shaped Stub Columns

Forty-six stub-column specimens fabricated from 35XF and 50XF sheet steels were tested in this study under different strain rates. Box-shaped stub columns were fabricated by connecting two identical hat sections through the unstiffened flanges. High-strength bolts (1/4-in. [6.4-mm] diameter) with washers were used for the fabrication of test specimens. The spacing of bolts satisfied the requirements of the AISI specification (*Specification* 1986). Prior to testing, both ends of the stub-column specimens were milled to ensure that they were flat and parallel.

The cross section of the box-shaped stub column is shown in Fig. 1. The webs of all hat sections were designed to be fully effective. Tables 3 and 4 give the average cross-sectional dimensions of stub-column specimens fabricated from 35XF and 50XF sheet steels. The strain rates used in the tests ranged from 10^{-4} to 0.1 in./in./sec (10^{-4} to 0.1 mm/mm/s).

Eight foil strain gages were used to measure strains at midheight of the stub-column specimens. For the stub columns with large *w/t* ratios, additional eight strain gages were mounted above and below the midheight of the stub column at a distance along the length of the column equal to one-half of the overall width of the stiffened element. The arrangement of strain gages is shown in Fig. 2.

I-Shaped Stub Columns

In this study, 51 I-shaped stub columns were tested to study the local-buckling and postbuckling strength of unstiffened elements of the 35XF and

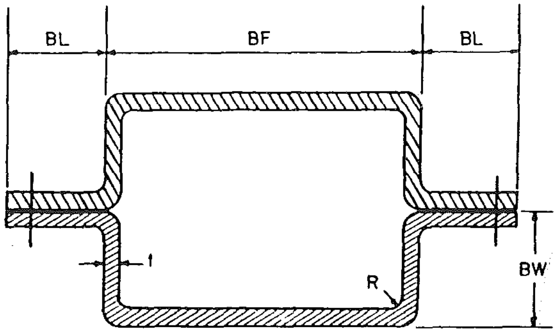

FIG. 1. Cross Section of Box-Shaped Stub Columns

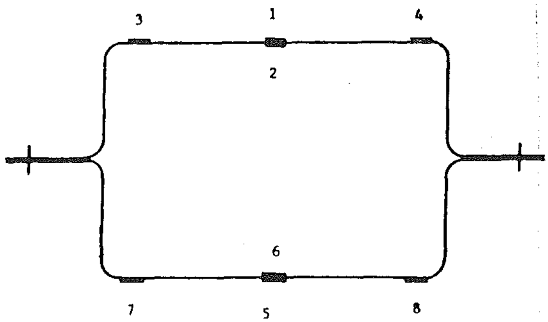

FIG. 2. Locations of Strain Gages at Midheight of Box-Shaped Stub Columns

50XF sheet steels using different strain rates. The strain rates used for the tests ranged from 10^{-5} to 0.1 in./in./sec (10^{-5} to 0.1 mm/mm/s). Fig. 3 shows the cross section of an I-shaped stub column. Tables 5 and 6 give the average cross-sectional dimensions of stub-column specimens fabricated from 35XF and 50XF sheet steels, respectively. The stub-column specimens were fabricated by adhesively bonding two identical channels back to back. Contact surfaces were paper sanded and cleaned with methyl alcohol and bonded by a thin layer of PC-7 epoxy. The webs of the channels were held together by C-clamps after glue was placed on the web. Thin wires (0.002-in. [0.05-mm] diameter) were placed between the channel webs to maintain uniform epoxy thickness. These C-clamps were removed after 24 hours. Great care was taken when the stub columns were fabricated. Prior to testing, the ends of stub-column specimens were milled flat and parallel.

Fourteen foil strain gages were used to measure strains at the midheight of stub-column specimens. The arrangement of strain gages is shown in Fig. 4.

Test Procedure and Test Results

All stub column specimens were tested in a 110-kip (489-kN) 880 material test system (MTS) using stroke (actuator displacement) as the control mode of machine operation to maintain a constant actuator speed. The speed of the actuator is equal to the slope of the function-generator programmed ramp. The data-acquisition system used in this study consists of 64 simul-

TABLE 3. Dimensions of Box-Shaped Stub Columns (35XF Sheet Steel)

Specification (1)	BF[a] (in.) (2)	BW[a] (in.) (3)	BL[a] (in.) (4)	w/t (5)	Gross area (sq. in.) (6)	Length (in.) (7)
1A1A	2.790	1.492	0.916	27.15	1.2060	12.03
1A1B	2.811	1.482	0.915	27.39	1.2060	12.02
1A2A	2.771	1.484	0.918	26.92	1.2010	12.03
1A2B	2.783	1.482	0.916	27.06	1.2060	12.03
1A3A	2.804	1.470	0.916	27.31	1.2009	12.03
1A3B	2.812	1.467	0.915	27.40	1.2009	12.03
1B1A	3.792	1.990	0.922	38.93	1.5477	14.99
1B1B	3.812	1.985	0.918	39.17	1.5480	13.97
1B2A	3.786	1.978	0.918	38.86	1.5412	13.84
1B2B	3.806	1.982	0.919	38.86	1.5463	13.94
1B3A	3.786	1.992	0.919	39.10	1.5463	13.84
1B3B	3.794	1.982	0.918	38.96	1.5440	13.94
1C1A	4.961	2.523	0.919	52.69	1.9266	15.06
1C1B	4.984	2.513	0.922	52.96	1.9282	15.06
1C2A	4.920	2.524	0.920	52.20	1.9203	14.81
1C2B	4.993	2.519	0.922	53.06	1.9317	15.12
1C3A	5.000	2.526	0.919	53.15	1.9343	15.09
1C3B	5.021	2.510	0.922	53.39	1.9334	15.00
1D1A	9.041	3.008	1.024	100.68	2.8207	29.91
1D1B	9.012	3.026	1.019	100.35	2.8203	29.92
1D2A	9.024	3.011	1.018	100.49	2.8169	29.93
1D2B	9.035	3.009	1.020	100.62	2.8188	29.94
1D3A	9.055	3.002	1.021	100.85	2.8202	29.95
1D3B	9.044	3.014	1.009	100.72	2.8183	29.91

[a]See Fig. 1.
Note: 1 in. = 25.4 mm; 1 kips = 4.448 kN; and 1 sq in. = 645.16 mm^2.

taneously sampling input channels. Two channels were connected to the MTS machine to record loads and actuator displacements during each test. Thirty channels were connected to a 2120 measurements group strain-gage conditioner and amplifier system to measure the strain-gage outputs. The test frequency or sampling rate depended on the total test time with a maximum of 25,000 readings per second for each channel. After the data were acquired, they were downloaded into a computer for analysis. A data general minicomputer was used to coordinate the electronic equipment and to store and analyze the test data.

Box-Shaped Stub Columns

Following fabrication of the specimen and placement of strain gages, the stub column was placed in the MTS testing machine. At the beginning of the test, a small preload was applied to the specimen for the purpose of checking the alignment. If necessary, thin layers of the aluminum foil were placed at the end of the specimen in the regions of low strain until the load was uniformly distributed over the whole cross section. The actuator speed was obtained from multiplying the selected strain rate by the overall length of the specimen. Because the maximum actuator speed is 2.5 in./sec (63.5 m/s), a strain rate higher than 0.1 in./in./sec (0.1 mm/mm/s) could not be

J. Struct. Eng., 1992, 118(11): 3151-3168

TABLE 4. **Dimensions of Box-Shaped Stub Columns (50XF Sheet Steel)**

Specimen (1)	BF^a (in.) (2)	BW^a (in.) (3)	BL^a (in.) (4)	w/t (5)	Gross area (sq. in.) (6)	Length (in.) (7)
1A1AX	2.229	1.963	0.923	22.89	1.1569	14.94
1A1BX	2.249	1.982	0.921	23.15	1.1652	14.99
1A2AX	2.249	1.960	0.921	23.15	1.1584	15.00
1A2BX	2.233	1.967	0.923	22.94	1.1587	14.95
1A3AX	2.245	1.963	0.927	23.10	1.1605	14.98
1A3BX	2.231	1.961	0.938	22.92	1.1612	14.95
1B1AX	3.173	1.969	0.926	35.15	1.3050	14.98
1B1BX	3.130	1.978	0.926	34.59	1.3012	14.97
1B2AX	3.123	1.983	0.919	34.50	1.2995	14.99
1B2BX	3.158	1.977	0.926	34.95	1.3052	15.01
1B3AX	3.159	1.979	0.921	34.97	1.3044	14.98
1B3BX	3.145	1.975	0.934	34.79	1.3050	14.94
1C1AX	4.529	1.967	0.923	52.76	1.5123	14.94
1C1BX	4.578	1.962	0.936	53.40	1.5223	14.94
1C2AX	4.552	1.968	0.928	53.06	1.5177	14.94
1C2BX	4.488	1.971	0.928	52.23	1.5087	14.93
1C3AX	4.445	1.972	0.923	51.67	1.5009	14.97
1C3BX	4.540	1.975	0.926	52.90	1.5174	14.96
1D1AX	8.012	2.719	1.014	97.99	2.3083	25.94
1D2AX	8.029	2.719	1.009	98.21	2.3094	25.92
1D3AX	8.013	2.725	1.018	98.01	2.3115	25.94
1D3BX	8.018	2.727	1.018	98.07	2.3129	25.92

[a]See Fig. 1.
Note: 1 in. = 25.4 mm; 1 kips = 4.448 kN; and 1 sq in. = 645.16 mm^2.

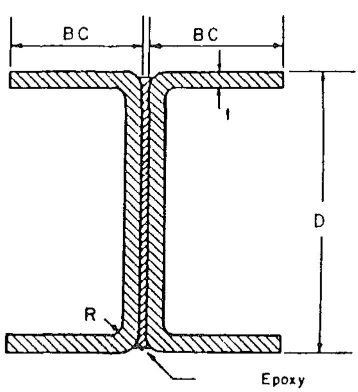

FIG. 3. Cross Section of I-Shaped Stub Columns

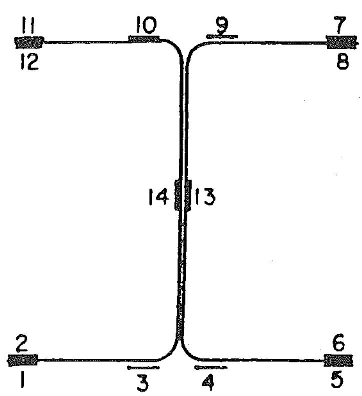

FIG. 4. Locations of Strain Gages at Midheight of I-Shaped Stub Columns

obtained. The strain rates used in the tests ranged from 10^{-4} to 0.1 in./in./sec (10^{-4} to 0.1 mm/mm/s).

The failure mode of the specimens varied with the width-to-thickness ratio of the compression flange. For stiffened elements with large *w/t* ratios

J. Struct. Eng., 1992, 118(11): 3151-3168

TABLE 5. Dimensions of I-Shaped Stub Columns (35XF Sheet Steel)

Specimen (1)	BC[a] (in.) (2)	D[a] (in.) (3)	w/t (4)	Gross area (sq. in.) (5)	Length (in.) (6)
2A1A	1.000	2.000	8.93	0.6220	7.90
2A1B	1.010	2.018	9.04	0.6285	7.97
2A2A	1.000	2.040	8.93	0.6288	7.95
2A2B	1.015	2.002	9.10	0.6275	7.94
2A3A	1.000	2.040	8.93	0.6288	7.98
2A3B	1.003	2.014	8.96	0.6254	7.94
2B1A	1.375	3.025	13.34	0.9238	9.95
2B1B	1.381	2.981	13.41	0.9184	9.97
2B2A	1.380	2.987	13.40	0.9190	9.96
2B2B	1.378	3.007	13.37	0.9217	9.94
2B3A	1.375	3.020	13.34	0.9229	10.01
2B3B	1.382	3.006	13.42	0.9229	9.99
2C0A	2.000	3.000	20.69	1.1320	14.00
2C1A	2.014	2.976	20.85	1.1327	14.00
2C1B	2.006	3.018	20.76	1.1371	13.94
2C2A	2.024	2.967	20.97	1.1346	14.09
2C2B	2.010	3.015	20.81	1.1380	13.95
2C3A	2.020	2.970	20.93	1.1337	14.06
2C3B	2.015	2.977	20.87	1.1332	13.91
2D1A	4.032	3.302	44.60	1.8743	23.92
2D1B	4.024	3.311	44.50	1.8731	23.94
2D2A	4.034	3.278	44.62	1.8709	23.92
2D2B	4.031	3.289	44.59	1.8717	23.93
2D3A	4.025	3.241	44.51	1.8615	23.90
2D3B	4.032	3.301	44.60	1.8741	23.92

[a]See Fig. 3.
Note: 1 in. = 25.4 mm; 1 kips = 4.448 kN; and 1 sq in. = 645.16 mm^2.

(cases C and D), local buckling always occurred in the elastic range. Due to the stress redistribution across the cross section of the compression flange, the edge stress of the stiffened element continued to increase until the maximum edge stress was reached and the specimen failed. For stiffened elements with medium w/t ratios (case B), the compression flange normally buckled in the inelastic range. Yield failure occurred in stiffened elements with small w/t ratios (case A). Figs. 5 and 6 are examples of locally buckled box-shaped and I-shaped stub columns. For the purpose of comparison, each plot of Figs. 7(*a*) and 7(*b*) presents three typical load-displacement curves for the specimens fabricated from 35XF and 50XF sheet steels having the same w/t ratio but tested under different strain rates.

I-Shaped Stub Columns

During the test, no bonding failure was observed prior to the attainment of the maximum load. The failure modes of stub-column specimens with unstiffened elements varied with the width-to-thickness ratios of the unstiffened compression flanges. The unstiffened flanges with large w/t ratios (cases C and D) showed large out of plane deformations, whereas the unstiffened compression flanges with small and medium w/t ratios (cases A

J. Struct. Eng., 1992, 118(11): 3151-3168

TABLE 6. Dimensions of I-Shaped Stub Columns (50XF Sheet Steel)

Specimen (1)	B^a (in.) (2)	D^a (in.) (3)	w/t (4)	Gross area (sq. in.) (5)	Length (in.) (6)
2A1AX	0.881	1.949	8.41	0.5218	6.97
2A1BX	0.879	1.958	8.38	0.5225	6.98
2A2AX	0.880	1.956	8.40	0.5228	6.98
2A2BX	0.879	1.956	8.38	0.5224	6.97
2A3AX	0.872	1.975	8.29	0.5232	6.99
2A3BX	0.877	1.962	8.36	0.5226	6.96
2B1AX	1.133	2.961	11.68	0.7553	8.99
2B1BX	1.127	2.992	11.60	0.7582	8.94
2B1CX	1.129	2.994	11.63	0.7593	8.99
2B2AX	1.125	2.999	11.58	0.7589	8.97
2B2BX	1.122	3.024	11.54	0.7616	9.00
2B2CX	1.121	2.987	11.53	0.7558	8.98
2B3AX	1.131	2.986	11.65	0.7586	9.00
2B3BX	1.119	2.994	11.50	0.7563	8.97
2C1AX	1.992	3.043	22.84	1.0327	14.94
2C1BX	1.984	3.064	22.73	1.0333	14.96
2C2AX	1.987	3.047	22.77	1.0316	14.94
2C2BX	1.986	3.057	22.76	1.0329	14.95
2C3AX	1.983	3.041	22.72	1.0295	14.97
2C3BX	1.988	3.055	22.79	1.0333	14.94
2D1AX	2.957	2.717	35.37	1.2796	17.94
2D1BX	2.954	2.717	35.33	1.2786	17.94
2D2AX	2.948	2.719	35.26	1.2772	17.94
2D2BX	2.945	2.722	35.21	1.2767	17.94
2D3AX	2.951	2.715	35.29	1.2774	17.94
2D3BX	2.940	2.725	35.15	1.2754	17.94

[a]See Fig. 3.
Note: 1 in. = 25.4 mm; 1 kips = 4.448 kN; and 1 sq in. = 645.16 mm^2.

and B) showed no noticeable waving until failure. Fig. 6 shows the local buckling mode developed in the stub-column specimen with a w/t ratio of 44.62. Each plot of Figs. 8(a) and 8(b) presents three typical load-displacement curves for the specimens fabricated from 35XF and 50XF sheet steels having the same w/t ratio but tested under different strain rates. The strain rates used in the tests ranged from 10^{-5} to 0.1 in./in./sec (10^{-5} to 0.1 mm/mm/s).

EVALUATION OF EXPERIMENTAL DATA

The results of tests obtained from this study were evaluated by comparing the tested failure loads with the predicted ultimate load-carrying capacities of stub columns based on the current AISI effective width equations and using: (1) Static yield stresses; and (2) dynamic yield stresses corresponding to the strain rates used in the tests. Also presented are the ratios of dynamic to static ultimate loads for stub columns having same dimensions but tested under different strain rates. It is well known that the cold-forming operation increases the yield stress and tensile strength of the steel in the corners of

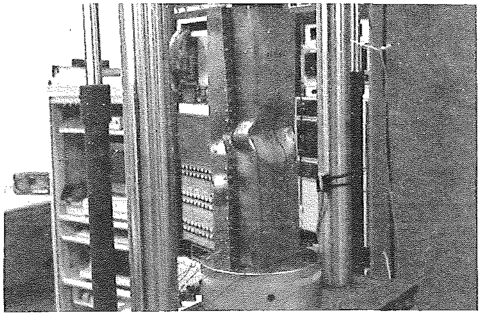

FIG. 5. Failure of Box-Shaped Stub Columns (Specimen 1D3BX)

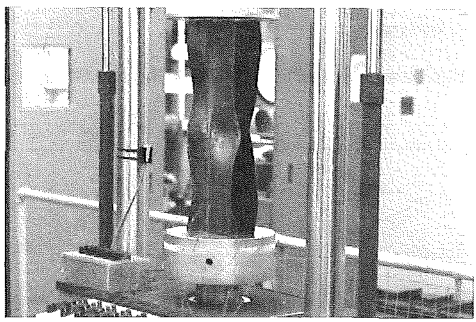

FIG. 6. Failure of I-Shaped Stub Columns (Specimen 2D2A)

cross sections. In order to consider the effect of cold work on the axial strength of the stub columns, comparisons are also made between the tested and predicted ultimate loads.

Box-Shaped Stub Columns

The box-shaped sections were designed and fabricated for stub-column tests to study the postbuckling strengths of stiffened elements. All stub columns were subjected to uniform compression, and overall column buckling was prevented by selecting the appropriate length. All webs of stub columns were designed to be fully effective on the basis of version 3 of the AISI *Automotive Steel Design Manual* (1986). According to the same reference, all unstiffened elements (BL) in the sections tested were fully effective.

Critical Local Buckling Load

The compression element of a stub column specimen may buckle locally in the elastic or inelastic range, depending on the w/t ratio of the compression element. The critical local buckling loads of stub columns can be computed by using the following equation:

$$P_{cr} = A_g f_{cr} \quad (1)$$

where f_{cr} = elastic or inelastic critical buckling stress, whichever is applicable; and A_g = gross cross-sectional area of the stub column.

J. Struct. Eng., 1992, 118(11): 3151-3168

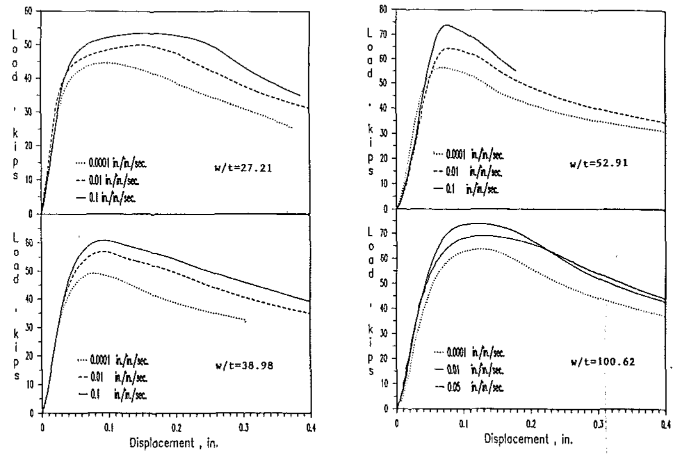

FIG. 7(*a*). Load-Displacement Curves for Box-Shaped Stub Columns (Using 35XF Sheet Steel)

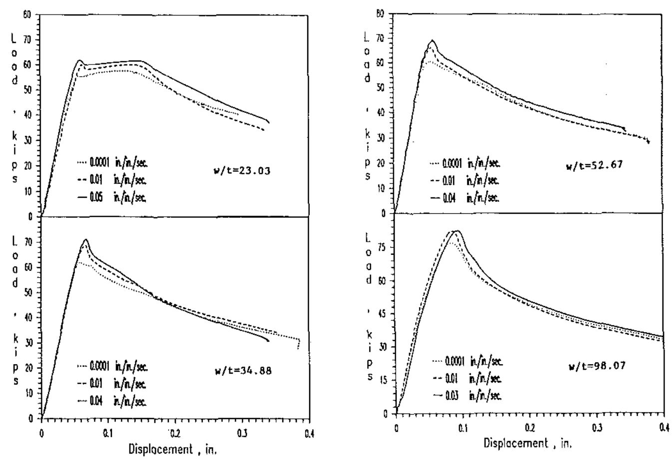

FIG. 7(*b*). Load-Displacement Curves for Box-Shaped Stub Columns (Using 50XF Sheet Steel)

The tested, critical local buckling loads were determined from load-strain relationships by using the modified strain-reversal method. The load-strain relationships showed that no local buckling occurred in the specimens with small or medium *w*/*t* ratios for both sheet steels used in the tests. Comparisons between the tested and predicted local critical buckling loads indicated that the predicted buckling loads for box-shaped stub columns fabricated from 50XF sheet steel are less conservative than the stub columns fabricated from 35XF sheet steel (Pan and Yu 1990).

Ultimate Load

A stub-column specimen is assumed to attain its ultimate load when the maximum edge stress in the stiffened element reaches the yield stress of the

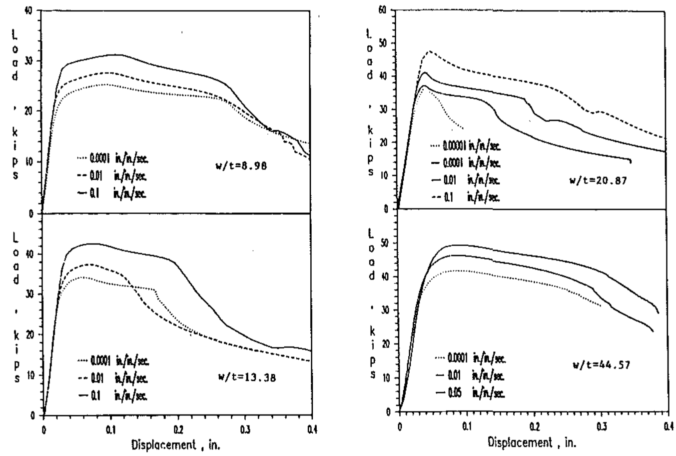

FIG. 8(*a*). Load-Displacement Curves for I-Shaped Stub Columns (Using 35XF Sheet Steel)

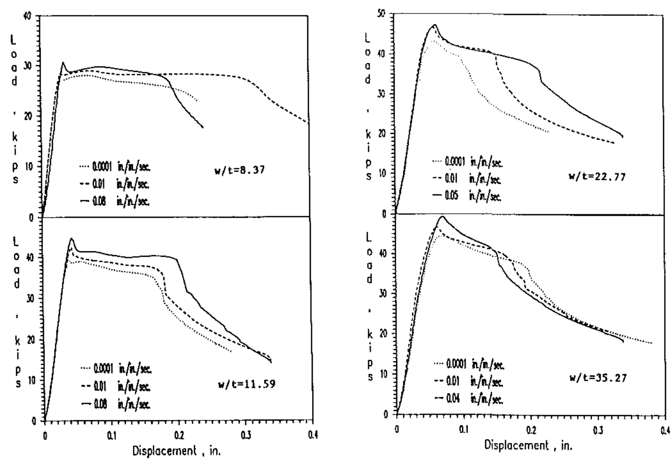

FIG. 8(*b*). Load-Displacement Curves for I-Shaped Stub Columns (Using 50XF Sheet Steel)

steel. The ultimate load can be calculated from the effective cross-sectional area of the stub column and the yield stress of steel as expressed in (6). The concept of effective design width [(2) and (3)] can be used to compute the effective cross-sectional area, i.e.

$$b = w \qquad \text{when } \lambda \leq 0.673 \quad \text{(2)}$$

$$b = \rho w \qquad \text{when } \lambda > 0.673 \quad \text{(3)}$$

where b = effective width of a compression element; w = flat width of a compression element;

$$\rho = \frac{1 - \frac{0.22}{\lambda}}{\lambda} \quad \text{(4)}$$

λ = a slenderness factor; and

$$\lambda = \frac{1.052}{\sqrt{k}} \left(\frac{w}{t}\right) \left(\sqrt{\frac{f}{E}}\right) \quad \text{(5)}$$

In (5) f = the edge stress; E = modulus of elasticity (29,500 ksi [203 kN/mm^2]); and k = plate buckling coefficient. Consequently, the ultimate load is

$$P_u = A_e F_y \quad \text{(6)}$$

where A_e = effective cross-sectional area of the stub column; and F_y = static or dynamic yield stress of steel.

According to the AISI *Specification for the Design of Cold-Formed Steel Structural Members* (1986), the strength of a compact section (i.e., $\rho = 1$) including the cold work of forming may be determined by substituting F_{ya} for F_y to compute the ultimate load, where F_{ya} is the average yield stress of the full section, and can be computed as follows:

$$F_{ya} = CF_{yc} + (1 - C)F_{yf} \quad \text{(7)}$$

where F_{ya} = average tensile yield stress of steel; C = ratio of the total corner cross-sectional area to the total cross-sectional area of the full section; F_{yf} = weighted average tensile yield stress of flat portions

$$F_{yc} = \frac{B_c F_{yv}}{\left(\frac{R}{t}\right)^m} \quad \text{(8)}$$

is the tensile yield stress of corners; and

$$B_c = 3.69 \left(\frac{F_{uv}}{F_{yv}}\right) - 0.819 \left(\frac{F_{uv}}{F_{yv}}\right)^2 - 1.79 \quad \text{(9)}$$

$$m = 0.192 \left(\frac{F_{uv}}{F_{yv}}\right) - 0.068 \quad \text{(10)}$$

R = inside bend radius; F_{yv} = tensile yield stress of virgin steel; and F_{uv} = ultimate tensile strength of virgin steel. Eq. (7) can be used only when $F_{uv}/F_{yv} \geq 1.2$, $R/t \leq 7$, and minimum included angle $\leq 120°$.

The predicted ultimate loads based on the applicable tensile yield stresses and the tested ultimate loads are presented in Table 7 for box-shaped stub columns fabricated from 35XF sheet steel. Table 8 presents the similar data for box-shaped stub columns fabricated from 50XF sheet steel. In both tables, the ultimate loads for the box-shaped stub columns with small w/t ratios ($w/t < 27.40$ in Table 7 and $w/t < 23.15$ in Table 8) were computed by considering the cold-work effect.

By comparing the mean values and standard deviations of $(P_u)_{test}/(P_u)_{comp}$ ratios listed in columns 6 and 7 of Tables 7 and 8, it can be seen that the computed ultimate loads using dynamic yield stresses are better than that

J. Struct. Eng., 1992, 118(11): 3151-3168

TABLE 7. Comparison of Computed and tested Failure Loads Based on Effective Width Formulas in *AISI Automotive Steel Design Manual* (1986) for Box-Shaped Stub Columns (35XF Sheet Steel) (Based on Tensile Yield Stress)

Specimen (1)	Strain rate (in. /in. /sec.) (2)	w/t (3)	$(P_u)_{comp}$ (kips) Based on $(F_y)_s$ (4)	$(P_u)_{comp}$ (kips) Based on $(F_y)_d$ (5)	$(P_u)_{test}$ (kips) (6)	Column 5/ column 3 (7)	Column 5/ column 4 (8)
1A1A	0.0001	27.15	44.28	44.28	46.12	1.04	1.04
1A1B	0.0001	27.39	44.28	44.28	44.89	1.01	1.01
1A2A	0.01	26.92	44.11	48.26	50.02	1.13	1.04
1A2B	0.01	27.06	44.13	48.29	49.29	1.12	1.02
1A3A	0.10	27.31	44.11	51.45	53.54	1.21	1.04
1A3B	0.10	27.40	44.11	51.45	54.37	1.23	1.06
1B1A	0.0001	38.93	50.73	50.73	49.19	0.97	0.97
1B1B	0.0001	39.17	50.68	50.68	53.54	1.06	1.06
1B2A	0.01	38.86	50.53	55.41	56.28	1.11	1.02
1B2B	0.01	39.10	50.64	55.52	57.01	1.13	1.03
1B3A	0.10	38.86	50.70	59.26	64.78	1.28	1.09
1B3B	0.10	38.96	50.60	59.13	60.87	1.20	1.03
1C1A	0.0001	52.69	58.92	58.92	56.76	0.96	0.96
1C1B	0.0001	52.96	58.88	58.88	56.52	0.96	0.96
1C2A	0.01	52.20	58.88	64.42	61.02	1.04	0.95
1C2B	0.01	53.06	58.96	64.48	64.58	1.10	1.00
1C3A	0.10	53.15	59.01	68.70	73.96	1.25	1.08
1C3B	0.10	53.39	58.89	68.56	69.27	1.18	1.01
1D1A	0.0001	100.68	68.58	68.58	63.85	0.93	0.93
1D1B	0.0001	100.35	68.72	68.72	63.90	0.93	0.93
1D2A	0.01	100.49	68.54	74.46	70.35	1.03	0.94
1D2B	0.01	100.62	68.55	74.78	69.22	1.01	0.93
1D3A	0.05	100.85	68.49	77.88	74.06	1.08	0.95
1D3B	0.05	100.72	68.48	77.87	72.45	1.06	0.93
Mean						1.084	0.999
Standard deviation						0.103	0.052

Note: Cold-work effect was considered in calculation of yield stresses for all six sections used in first group (specimens 1A1A–1A3B). 1 in./in./sec = 1 mm/mm/s; 1 kips = 4.448 kN.

using static yield stress for 35XF steel. The predicted ultimate loads for box-shaped stub columns fabricated from 50XF sheet steel were found to be slightly less conservative than those fabricated from 35XF sheet steel. It is also noted that the tested ultimate load increases with the strain rate for specimens having the same w/t ratio.

I-Shaped Stub Columns

The I-shaped stub columns were designed and fabricated to study the postbuckling strength of unstiffened elements under different strain rates. All the stub columns were subjected to uniform compression, and overall column buckling was prevented by selecting the appropriate length. The thickness of the web was twice the thickness of the unstiffened compression flange because the webs of two channels were glued together.

J. Struct. Eng., 1992, 118(11): 3151-3168

TABLE 8. Comparison of Computed and Tested Failure Loads Based on Effective Width Formulas in AISI *Automotive Steel Design Manual* (1986) for Box-Shaped Stub Columns (50XF Sheet Steel) (Based on Tensile Yield Stress)

Specimen (1)	Strain rate (in./in./sec) (2)	w/t (3)	$(P_u)_{comp}$ (kips) Based on $(F_y)_s$ (4)	$(P_u)_{comp}$ (kips) Based on $(F_y)_d$ (5)	$(P_u)_{test}$ (kips) (6)	Column 5/ column 3 (7)	Column 5/ column 4 (8)
1A1AX	0.0001	22.89	62.91	62.91	57.89	0.92	0.92
1A1BC	0.0001	23.15	63.32	63.32	57.65	0.91	0.91
1A2AX	0.01	23.15	62.99	65.49	59.82	0.95	0.91
1A2BX	0.01	22.94	63.00	65.48	60.23	0.96	0.92
1A3AX	0.05	23.10	63.10	66.74	63.95	1.01	0.96
1A3BX	0.05	22.92	63.13	66.77	62.04	0.98	0.93
1B1AX	0.0001	35.49	63.29	63.29	62.19	0.98	0.98
1B1BX	0.0001	34.59	63.30	63.30	61.75	0.98	0.98
1B2AX	0.01	34.50	63.25	65.69	68.88	1.09	1.05
1B2BX	0.01	34.96	63.37	65.81	67.86	1.07	1.03
1B3AX	0.04	34.97	63.33	66.72	71.42	1.13	1.07
1B3BX	0.04	34.79	63.43	66.82	71.52	1.13	1.07
1C1AX	0.0001	52.76	65.86	65.86	60.09	0.91	0.91
1C1BC	0.0001	53.40	66.04	66.04	60.67	0.92	0.92
1C2AX	0.01	53.06	65.98	68.42	64.00	0.97	0.94
1C2BX	0.01	52.23	65.94	68.30	66.44	1.01	0.97
1C3AX	0.04	51.67	65.82	69.21	66.54	1.01	0.96
1C3BX	0.04	52.90	66.04	69.43	69.47	1.05	1.00
1D1AX	0.0001	97.99	81.15	81.15	76.94	0.95	0.95
1D2AX	0.01	98.21	81.08	84.05	82.22	1.01	0.98
1D3AX	0.03	98.01	81.30	85.20	82.46	1.01	0.97
1D3BX	0.03	98.07	81.33	85.23	80.85	0.99	0.95
Mean	—	—	—	—	—	0.997	0.967
Standard deviation	—	—	—	—	—	0.065	0.050

Note: Cold-work effect was considered in calculation of yield stresses for all six sections used in first group (specimens 1A1AX–1A3BX). 1 in./in./sec = 1 mm/mm/s; and kips = 4.448 kN.

Critical Local Buckling Load

The critical local buckling load of I-shaped stub-column specimen with unstiffened compression flanges can be calculated by using (1), except that f_{cr} is the critical local buckling stress of the unstiffened flange. Similar to stiffened elements, unstiffened elements of stub columns may buckle locally in the elastic or inelastic ranges, depending on the w/t ratio of the compression element. Comparisons between the tested and predicted local critical buckling loads were made by Pan and Yu (1990).

Ultimate Load

The ultimate load-carrying capacity (P_u) of stub-column specimens can be calculated from (6). Comparisons between the tested ultimate loads and the predicted values based on tensile yield stresses are presented in Table 9 for 35XF sheet steel and in Table 10 for 50XF sheet steel, in which the cold-work effect was considered in the computations of ultimate loads for

TABLE 9. Comparison of Computed and Tested Failure Loads Based on Effective Width Formulas in AISI *Automotive Steel Design Manual* (1986) for I-Shaped Stub Columns (35XF Sheet Steel) (Based on Tensile Yield Stress)

			$(P_u)_{comp}$ (kips)				
Specimen (1)	Strain rate (in./in./sec) (2)	w/t (3)	Based on $(F_y)_s$ (4)	Based on $(F_y)_d$ (5)	$(P_u)_{test}$ (kips) (6)	Column 5/column 3 (7)	Column 5/column 4 (8)
2A1A	0.0001	8.93	22.77	22.77	25.26	1.11	1.11
2A1B	0.0001	9.04	22.98	22.98	25.35	1.10	1.10
2A2A	0.01	8.93	22.99	25.17	26.04	1.13	1.03
2A2B	0.01	9.10	22.95	25.12	27.70	1.21	1.10
2A3A	0.10	8.93	22.99	26.83	31.41	1.37	1.17
2A3B	0.10	8.96	22.88	26.70	29.41	1.29	1.10
2B1A	0.0001	13.34	29.97	29.97	34.20	1.14	1.14
2B1B	0.0001	13.41	29.75	29.75	34.20	1.15	1.15
2B2A	0.01	13.40	29.78	32.59	36.30	1.22	1.11
2B2B	0.01	13.37	29.88	32.70	37.52	1.26	1.15
2B3A	0.10	13.34	29.94	34.88	41.67	1.39	1.19
2B3B	0.10	13.42	29.90	34.82	42.70	1.43	1.23
2C0A	0.00001	20.69	31.77	31.09	36.30	1.14	1.17
2C1A	0.0001	20.85	31.67	31.67	37.23	1.18	1.18
2C1B	0.0001	20.76	31.88	31.88	37.66	1.18	1.18
2C2A	0.01	20.97	31.63	34.43	41.28	1.31	1.20
2C2B	0.01	20.81	31.88	34.70	41.52	1.30	1.20
2C3A	0.10	20.93	31.64	36.53	47.92	1.51	1.31
2C3B	0.10	20.87	31.67	36.57	46.16	1.46	1.26
2D1A	0.0001	44.60	35.35	35.35	41.72	1.18	1.18
2D1B	0.0001	44.50	35.39	35.39	41.04	1.16	1.16
2D2A	0.01	44.62	35.21	38.19	46.31	1.32	1.21
2D2B	0.01	44.59	35.27	38.26	44.94	1.27	1.17
2D3A	0.05	44.51	35.00	39.46	48.66	1.39	1.23
2D3B	0.05	44.60	35.34	39.85	49.39	1.40	1.24
Mean	—	—	—	—	—	1.264	1.171
Standard deviation	—	—	—	—	—	0.120	0.060

Note: Cold-work effect was considered in calculation of yield stresses for all six sections used in first group (specimens 2A1A–2A3B). 1 in./in./sec = 1 mm/mm/s; and 1 kips = 4.448 kN.

the I-shaped stub columns with w/t ratios less than 9.1. It can be seen that the computed ultimate loads using the dynamic yield stresses are better than the computed loads using the static yield stress. Similar to the results for studying box-shaped stub columns, the predicted ultimate loads for I-shaped stub columns fabricated from 50XF sheet steel are slightly less conservative than the stub columns fabricated from 35XF sheet steel. The tested ultimate load increases with strain rate for the specimens having the same w/t ratio. Comparisons between the predicted ultimate loads based on the compressive static and dynamic yield stresses and the tested ultimate loads were also made by Pan and Yu (1990).

TABLE 10. Comparison of Computed and Tested Failure Loads Based on Effective Width Formulas in AISI *Automotive Steel Design Manual* (1986) for I-Shaped Stub Columns (50XF Sheet Steel) (Based on Tensile Yield Stress)

Specimen (1)	Strain rate (in./in./sec) (2)	w/t (3)	$(P_u)_{comp}$ (kips) Based on $(F_y)_s$ (4)	$(P_u)_{comp}$ (kips) Based on $(F_y)_d$ (5)	$(P_u)_{test}$ (kips) (6)	Column 5/ column 3 (7)	Column 5/ column 4 (8)
2A1AX	0.0001	8.41	28.66	28.66	28.04	1.00	1.00
2A1BX	0.0001	8.38	28.70	28.70	28.16	0.98	0.98
2A2AX	0.01	8.40	28.70	29.82	29.02	1.01	0.97
2A2BX	0.01	8.38	28.69	29.80	29.43	1.03	0.99
2A3AX	0.08	8.29	28.72	30.54	30.75	1.07	1.01
2A3BX	0.08	8.36	28.70	30.52	30.95	1.08	1.01
2B1AX	0.0001	11.68	36.42	36.42	39.72	1.09	1.09
2B1BX	0.0001	11.60	36.63	36.63	39.18	1.07	1.07
2B1CX	0.00001	11.63	36.65	36.19	39.47	1.08	1.09
2B2AX	0.01	11.58	36.67	38.06	42.60	1.16	1.12
2B2BX	0.01	11.54	36.84	38.24	42.55	1.15	1.11
2B2CX	0.001	11.53	36.55	37.17	41.77	1.14	1.12
2B3AX	0.08	11.65	36.60	38.82	45.07	1.23	1.16
2B3BX	0.08	11.50	36.59	38.82	44.94	1.23	1.16
2C1AX	0.0001	22.84	39.55	39.55	43.62	1.10	1.10
2C1BX	0.0001	22.73	39.70	39.70	43.97	1.11	1.11
2C2AX	0.01	22.77	39.57	40.98	46.70	1.18	1.14
2C2BX	0.01	22.76	39.65	41.06	46.26	1.17	1.13
2C3AX	0.05	22.72	39.52	41.56	47.34	1.20	1.14
2C3BX	0.05	22.79	39.63	41.69	46.85	1.18	1.12
2D1AX	0.0001	35.37	37.99	37.99	44.06	1.16	1.16
2D1BX	0.0001	35.33	37.99	37.99	44.50	1.17	1.17
2D2AX	0.01	35.26	38.00	39.30	46.75	1.23	1.19
2D2BX	0.01	35.21	38.02	39.32	47.58	1.25	1.21
2D3AX	0.04	35.29	37.97	39.78	49.39	1.30	1.24
2D3BX	0.04	35.15	38.04	39.85	48.95	1.29	1.23
Mean	—	—	—	—	—	1.141	1.109
Standard deviation	—	—	—	—	—	0.087	0.077

Note: Cold-work effect was considered in calculation of yield stresses for all six sections used in first group (specimens 2A1AX–2A3BX). 1 in./in./sec = 1 mm/mm/s; and 1 kips = 4.448 kN.

Conclusions

The following conclusions can be drawn from a study of the effect of strain rate on structural strength of cold-formed steel stub columns:

1. For all cases investigated in this phase of study, the ultimate loads of box-shaped and I-shaped stub columns fabricated from 35XF and 50XF sheet steels increased with increasing strain rates.
2. The test results of the stub columns fabricated from 35XF and 50XF sheet steels indicated that the present effective width design method provides good predictions for stub columns with locally buckled stiffened compression

J. Struct. Eng., 1992, 118(11): 3151-3168

elements subjected to different strain rates. For stub columns with locally buckled unstiffened compression elements, the present design method provides conservative predictions.

3. From the test results on box-shaped and I-shaped stub columns, the predicted ultimate loads for the stub columns fabricated from 50XF sheet steel were found to be slightly less conservative than the stub columns fabricated from 35XF sheet steel.

4. In general, the dynamic yield stress provides a better prediction than static yield stress.

5. For the compact box-shaped and I-shaped stub columns with small w/t ratios (i.e., $\rho = 1$), a better prediction of ultimate loads can be obtained by considering the cold-work effect. However, the cold-work effect may be neglected for stub columns with large w/t ratios (i.e., $\rho < 1$).

6. The tensile yield stress, rather than the compressive yield stress, may be used to predict the load-carrying capacity of stub columns.

Acknowledgments

This investigation was sponsored by the American Iron and Steel Institute (AISI). The technical guidance provided by the AISI task force on automotive structural design, under the chairmanship of S. J. Errera, the AISI staff, and A. L. Johnson, is gratefully acknowledged. Materials used in the experimental study were donated by LTV Steel Co. and Inland Steel Co.

Appendix I. References

Abramowicz, W., and Jones, N. (1984). "Dynamic axial crushing of square tubes." *Int. J. Impact Engrg.*, 2(2), 263–281.

Aspden, R. J., and Campbell, J. D. (1966). "The effect of loading rate on the elasto-plastic flexure of steel beams." *Proc. of Royal Soc. of London*, Royal Society of London, A290, 266–285.

Automotive steel design manual. (1986). American Iron and Steel Inst., Washington, D.C.

Bodner, S. R., and Symonds, P. S. (1962). "Experimental and theoretical investigation of the plastic deformation of cantilever beams subjected to impulsive loading." *J. Appl. Mech.*, 29, Dec., 719–728.

Forrestal, M. J., and Wesenberg, D. L. (1977). "Elastic plastic response of simply supported 1018 steel beams to impulse loads." *J. Appl. Mech.*, 44, Dec., 779–780.

Galambos, T. V., ed. (1988). *Guide to stability design criteria for metal structures.* 4th Ed., John Wiley and Sons, New York, N.Y.

Hoff, N. (1965). "Dynamic stability of structures." *Proc. Int. Conference on Dynamic Stability of Structures*, Northwestern University, Evanston, Ill.

Johnson, A. L., and Winter, G. (1966). "The structural performance of austenitic stainless steel members." *Report No. 327,* Cornell Univ., Ithaca, N.Y.

Kassar, M., and Yu, W. W. (1992). "Effect of strain rate on material properties of sheet steels." *J. Struct. Engrg.*, ASCE, 118(11), 3136–3150.

Logue, J. M. (1971). "Experimental study of thin-walled columns subjected to impact loading," MS thesis, Carnegie-Mellon University, Pittsburgh, Pa.

Mahmood, H. F., and Paluszny, A. (1984). "Axial collapse of thin wall cylindrical column." *Fifth Int. Conference on Vehicular Struct. Mech. Proc.*, Society of Automotive Engineers, 45–56.

Meier, J. H. (1945). "On the dynamic of elastic buckling." *J. Aerosp. Sci.*, 12(4), 443–440.

Pan, C. L., and Yu, W. W. (1990). "Structural strength of cold-formed steel members

under dynamic loads." *Fifteenth Progress Report, Civil Engineering Study 90-3*, Univ. of Missouri–Rolla, Rolla, Missouri.
Rawlings, B. (1963). "The dynamic behavior of steel in pure flexure." *Proc. Royal Soc.*, Royal Society of London, 275, Mar., 528–543.
Roberts, T. M. (1972). "The response of steel struts to impact overload," PhD thesis, University of Sheffield, U.K.
Specification for the Design of Cold-Formed Steel Structural Members. (1986). American Iron and Steel Inst., Washington, D.C.
Wierzbicki, T. (1977). "Dynamic crushing of strain rate sensitive box columns." *SAE Second Int. Conference on Vehicle Struct. Mech.*, Society of Automotive Engineers, Warrendale, Pa.
Wierzbicki, T., and Abramowicz, W. (1979). "Crushing of thin-walled strain-rate sensitive structures." *Dynamic and crushing analysis of plastic structures, Euromech Colloquium No. 121*, Aug.

Appendix II. Notation

The following symbols are used in this paper:

A_e = effective cross-sectional area of stub columns;
A_g = gross cross-sectional area of stub columns;
b = effective width of compression element;
C = ratio of total corner cross-sectional area to total cross-sectional area of full section;
E = modulus of elasticity of steel (29,500 ksi [203 kN/mm^2]);
f_{cr} = critical local buckling stress;
F_{pr} = proportional limit;
F_y = yield stress;
F_{ya} = average tensile yield stress of steel;
F_{yc} = corner yield stress;
F_{yf} = weighted average tensile yield stress of flat portions;
F_{yv} = tensile yield stress of virgin steel;
$(F_y)_d$ = dynamic yield stress;
$(F_y)_s$ = static yield stress;
F_u = ultimate tensile strength;
F_{uv} = ultimate tensile strength of virgin steel;
P_{cr} = critical local buckling load;
P_u = ultimate load;
R = inside bend radius;
t = thickness of element;
w = flat width of compression element;
λ = slenderness factor; and
ρ = reduction factor.

J. Struct. Eng., 1992, 118(11): 3151-3168